Perpendicular transport in Fe/Ge model heterostructures

P. Weinberger
Center for Computational Materials Science, TU Wien, Getreidemarkt 9/158, A-1060 Wien, Austria

L. Szunyogh
Center for Computational Materials Science, TU Wien, Getreidemarkt 9/158, A-1060 Wien, Austria
and Department of Theoretical Physics, Budapest University for Technology and Economics, Budafoki út 8, 1521 Budapest, Hungary

C. Blaas
Center for Computational Materials Science, TU Wien, Getreidemarkt 9/158, A-1060 Wien, Austria

C. Sommers
Laboratoire de Physique des Solides, Université de Paris-Sud, 91405 Orsay Cedex, France
(Received 7 December 2000; revised manuscript received 12 July 2001; published 22 October 2001)

Based on the Kubo-Greenwood equation as formulated for layered systems, an approach is discussed that allows us to separate the resistance of the current leads from that of the region whose resistance we wish to calculate for current perpendicular to the plane of the layers. By applying this approach to Fe/Ge/Fe model structures related to the parent lattice of bcc Fe we find that at least nine layers of the magnetic electrodes should be considered as being part of the calculation in order to perform such a separation. With different structures in the Ge spacer, we find that the concentration of vacancies plays a crucial role for the existence of a sizeable magnetoresistance (MR), while the actual structure in the spacer seems to be of less importance. Depending on the type of structure and the number of spacer layers (in a typical regime of 6–21 layers) the MR for ordered structure varies between 35% and 45%. Vacancy concentrations of more than 10%, however, wipe out the MR completely. Interdiffusion at the Fe/Ge interfaces produces very similar effects.

DOI: 10.1103/PhysRevB.64.184429 PACS number(s): 75.30.Gw, 75.70.Ak, 75.70.Cn

I. INTRODUCTION

The Kubo formalism has been successfully applied to calculate the magnetotransport properties of magnetic multilayers when the current is in the plane of the layers (CIP); for this geometry the electric field is the same throughout the structure, and one can write[1,2]

$$\rho_{CIP}=\sigma_{CIP}^{-1}, \tag{1}$$

where

$$\sigma_{CIP}=\frac{1}{L}\int\int \sigma(z,z')dzdz'. \tag{2}$$

Here $\sigma(z,z')$ is the conductivity that relates the current at z when the field is given at z', where z and z' are along the growth direction of the multilayer, and L is the overall length of the structure for which the conductivity is calculated. For perpendicular transport, i.e., current perpendicular to the plane of the layers (CPP), the electric field is not uniform from layer to layer, and there are several ways of proceeding. One can use the Landauer-Büttiker or Caroli formalisms which do not require one to know the electric fields at each point in the multilayer, or as the current is independent of z in the steady state one can continue to use the Kubo formalism by writing the resistivity as[1,2,4]

$$\rho_{CPP}=\frac{1}{L}\int\int \rho(z,z')dzdz', \tag{3}$$

where $\rho(z,z')$ is the inverse of $\sigma(z,z')$ as defined by

$$\int \sigma(z,z'')\rho(z'',z')dz''=\delta(z-z'). \tag{4}$$

The sheet resistance r and resistance R are then defined by the relations

$$r=AR=L\rho_{CPP}=\int\int \rho(z,z')dzdz', \tag{5}$$

where A is the unit area. In the Caroli formalism one can calculate the resistance for a section of a multilayer across which one specifies the potential drop; however, in the Landauer and Kubo formalisms the electric field must vanish at the layers which bound the section.[5]

The Kubo formalism for the conductivity has vertex corrections that come from different sources,[1,4] e.g., from replacing the impurity averages over two electron propagators as the product of impurity averaged one-electron propagators, and from the varying electric fields from layer to layer that enter when one drives currents across the layers. The latter type of vertex corrections are accounted for as follows: we start by inverting the conductivity relation so as to write the electric field $E(z)$ at one point in terms of a two point resistivity function $\rho(z,z')$ and the current at another point $j(z')$. For further discussions we refer the reader to, e.g., Ref. 4. In the steady state the current is independent of z', and we account for this type of vertex correction by imposing current conservation for CPP, i.e., we find the resistance for perpendicular transport. The remaining vertex corrections

are similar to those encountered for CIP; while they are difficult to determine for layered structures they have been estimated to be quite small in the few cases in which we have been able to calculate them.[6,7]

As we have used the Kubo formalism extensively for CIP it is particularly convenient for us to use it for perpendicular transport; the complication lies in inverting the two-point conductivity function. In particular it is unclear over what region of z,z',z'' one must perform the calculation to obtain a reliable estimate of the resistivity. Clearly one has to go far enough away from the section of a multilayered structure whose resistance we are trying to calculate for the electric fields arising from charge and spin accumulation to vanish, i.e., we should only splice the sample in whose resistance we are interested in regions where the electric field due to the accumulation vanishes. To achieve this one wants to know the following: (1) How many layers of lead material have to be considered in the self-consistent solution of the electronic structure to accurately determine the charge and spin redistribution (the Madelung potentials) arising from the varying electronic properties of the layers? (2) How many layers of lead material have to be considered in the calculation of transport properties (the size of the conductivity matrix to be inverted) so as to properly account for the charge and spin accumulation when the current is driven across the region with the charge and spin redistribution so as to obtain a resistance that is independent of the number of lead layers chosen. Therefore, we have to determine how many layers to include in a Kubo calculation to be sure one has included all the layers with charge and spin redistribution and current driven accumulations in the section of a multilayer whose resistance we are calculating, so that the electric field vanishes across the layers bounding the outer layers of the section. We call this the problem of separating or splicing the leads from the ''disordered region'';[5] it is present in any kind of Landauer-Büttiker-type or related approach, just as well as in supercell approaches that make use of three-dimensional periodicity.

Here we will resolve this question for perpendicular transport in metallic multilayers, where the problem of separating the region of interest from the leads enters. For tunnel junctions one immediately knows how to do this separation and one can calculate the resistance of the barrier (spacer) layer separately from the electrodes, because the resistance of the barrier is overwhelmingly larger than that of the electrodes. In other words the resistors in series model is applicable for tunnel junctions, while it should not be applied *a priori* to metallic multilayers. The spacer we have chosen, Ge, is metallic for the thicknesses, the structure, and the lattice constant we use; however, for other structures and lattice spacings Ge can be semiconducting. For this reason we use the term ''heterostructure,'' which is associated with semiconductors, rather than ''multilayers,'' which is associated with metals. Thus, in addition to the problem of knowing what part of the leads to include, there are two additional problems that should be addressed for spacer materials which are putatively semiconductors, namely (a) the actual structure of the spacer material, and (b) the degree of interdiffusion at the interfaces. For metal-semiconductor heterostructures, sometimes called tunnel junctions, very little is known about the actual structure of the barrier region. The few studies that addressed this question (see for example Ref. 8), mostly stated that an amorphous layer of ''semiconductor material'' was deposited or produced. Future theoretical investigations may shed some light on the question whether a 10–20 Å thick layer of Si, Ge or GaAs really deserves the label semiconductor (and therefore tunnel junction) or not, i.e., whether there is a (''local'') gap between valence and conduction bands for such thin barriers. It should be noted that as long as the actual structure in such spacer materials is unknown, any assumed crystal structure can only serve as a model: a heterostructure does not simply consist of a combination of two bulk materials.

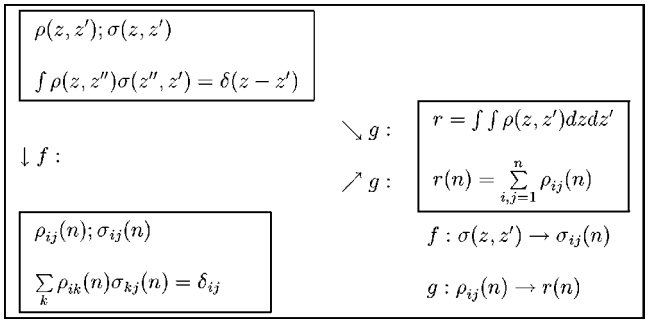

FIG. 1. Mapping of the two-point conductivity onto the zz component of the conductivity tensor for a layered system.

In this paper we describe a practical scheme for calculating the resistance for perpendicular transport across a metallic heterostructure (multilayer) that can account for interdiffusion at interfaces and alloying in both the electrodes and the spacer parts of the structure. In all cases investigated the fully relativistic spin-polarized screened Korringa-Kohn-Rostoker method[9–11] was applied in the context of the (inhomogeneous) coherent potential approximation (CPA) for layered systems[12] to obtain local-density-approximation effective potentials and effective exchange fields self-consistently. These in turn were used as input for the electric transport calculations, which also are based on a relativistic spin-polarized approach[13] and the CPA. For all transport calculations reported in here the occurring surface Brillouin–zone (SBZ) integrations were carried out using 1830 $k_\parallel$ points in the irreducible part of the SBZ.[14]

II. THEORETICAL APPROACH

In the following the conductivity tensor $\sigma(z,z')$ as defined in Eq. (2) is mapped (f:) onto the (zz components of the) conductivity tensor for a layered system,[12] $\sigma_{ij}(n),i,j=1,n$, with i and j denoting planes of atoms, such that the algebraic structure as defined by Eq. (4) is conserved (see in particular the scheme displayed in Fig. 1). Clearly enough the sheet resistance r then serves as measure (g:) for the mapping f, since according to the Cauchy convergence criterion, the integral in Eq. (5) can be replaced by a sum, i.e., by $r(n)$, if and only if

$$|r - \lim_{n\to\infty} r(n)| < \Delta, \quad n \in \mathbb{N}^+ \tag{6}$$

or

$$|r(n+m)-r(n)|<\Delta, \quad n,m\in\mathbb{N}^+, \tag{7}$$

where Δ is an infinitesimal small number.

Since for technical reasons (k-space integrations, surface Green's function, etc.) the elements of the $\sigma_{ij}(n)$ matrix[12] can only be calculated using a small imaginary part δ to the Fermi energy, the sheet resistance for a given magnetic configuration $\mathcal{C}$ is defined by

$$r(C;n)=\lim_{\delta\to 0} r(C;n;\delta), \tag{8}$$

where

$$r(C;n;\delta)=\sum_{i,j=1}^{n} \rho_{ij}(C;n;\delta). \tag{9}$$

In addition to this sheet resistance layer-resolved sheet resistances $r_i(n)$ can be defined

$$r_i(\mathcal{C};n;\delta)=\sum_{j=1}^{n} \rho_{ij}(\mathcal{C};n;\delta). \tag{10}$$

This qualitatively relates the electric field in layer i to the steady state current (CPP) which is independent of the layer index j. It should be noted, however, that only $r(C;n;\delta)$ in Eq. (9) is well defined. The layer-resolved sheet resistances are useful illustrative quantities in pursuing the question from which part of a layered system the main contributions to the sheet resistance of a given magnetic configuration arise.

As the sheet resistance $r(C;n;\delta)$ depends on both the number of layers n and the imaginary part of the Fermi energy δ in the following the properties of $r(C;n;\delta)$ with respect to these two parameters are first investigated for homogeneous metallic systems (the lead part of a heterostructure) and only then for heterostructures.

A. Homogeneous metallic systems (leads)

1. Layer dependence

In principle, for a large enough n $(n\geqslant n_0)$ and (because of) a given imaginary part δ of the complex Fermi energy $\epsilon_F+i\delta$, the corresponding sheet resistance $r(\mathcal{C};n;\delta)$ can be thought to vary linearly with n,

$$k_1(\mathcal{C};\delta)=\frac{r(\mathcal{C};n+m;\delta)-r(\mathcal{C};n;\delta)}{m}, \quad m,n\in\mathbb{N}^+, \tag{11}$$

i.e., the following relation can be assumed:

$$r(\mathcal{C};n;\delta)=r_0(\mathcal{C};\delta)+nk_1(\mathcal{C};\delta), \tag{12}$$

with $r_0(\mathcal{C};\delta)$ being the value of the linear form defined by Eq. (11) at $n=0$.

In the top part of Fig. 2 the sheet resistance $r(\mathcal{C};n;\delta)$ for bcc Fe(100)/Fe$_n$/Fe(100) is shown for three values of δ by varying n in terms of $N-m$, $N=45$, whereby $\mathcal{C}$ trivially refers to the ferromagnetic configuration. As can be seen for $n\geqslant 9$, $r(\mathcal{C};n;\delta)$ indeed vary linearly with n. According to this part of Fig. 2, n_0 ought to be at least 9 in order to yield a linear behavior. The rapid falloff for $n<n_0$ reflects the fact that the size of the $\sigma_{ij}(\mathcal{C};n;\delta)$ matrix to be inverted becomes too small: for $n=1$ only a diagonal element, namely $\sigma_{ii}(\mathcal{C};n)$ survives. In the lower part of Fig. 2 the extrapolation defined in Eq. (12) is performed numerically for $n_0\leqslant n \leqslant 45$, $n_0=12$.

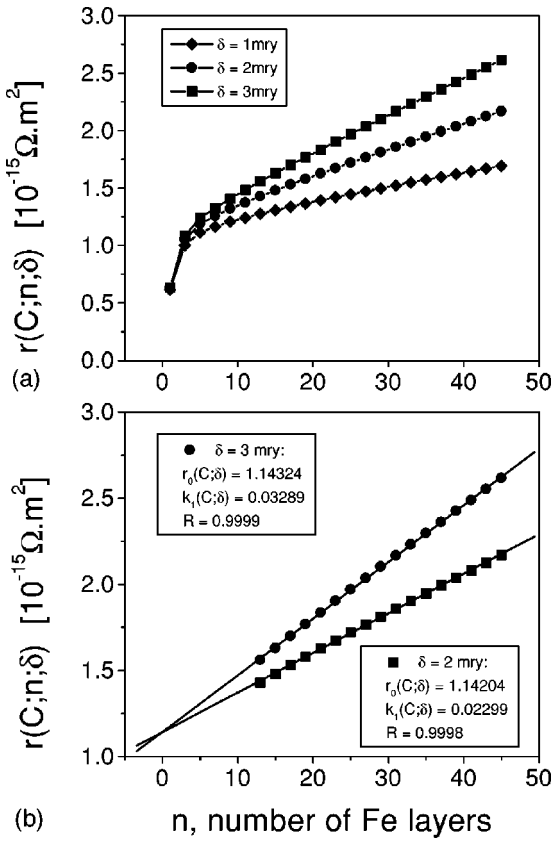

FIG. 2. Top: Variation of the sheet resistance $r(\mathcal{C};n;\delta)$ for ferromagnetic bcc Fe(100)/Fe$_n$/Fe with respect to n for three values of the imaginary part δ of the Fermi energy. Bottom: Numerical extrapolation (full line) of the linear regime of the sheet resistance $r(\mathcal{C};n;\delta)$ for ferromagnetic bcc Fe(100)/Fe$_n$/Fe. $r_0(\mathcal{C};\delta)$ and $k_1(\mathcal{C};\delta)$ refer to the value of $r(\mathcal{C};n;\delta)$ at $n=0$ and the slope, respectively. R is the quality of fitting.

In Fig. 3 again the variation of $r(\mathcal{C};n;\delta)$ with $n=N-m$ is shown—this time, however, by comparing the values obtained from different starting values N. As can be seen for $n=N-m>n_0$ one obtains the same linear behavior for $N=45$ and 60. The reason for this independence from N can be read off from the lower part of Fig. 3, where the corresponding layer-resolved sheet resistances [see Eq. (10)], are displayed: in the very interior of the systems Fe(100)/Fe$_N$/Fe(100) these quantities are virtually constant. Large variations only occur in the first and last nine layers.

2. Dependence on the imaginary part of the Fermi energy

Investigating now for a given value of n the dependence of $r(\mathcal{C};n;\delta)$ with respect to δ one can see from the top of Fig. 4 that $r(\mathcal{C};n,\delta)$ also varies linearly in δ:

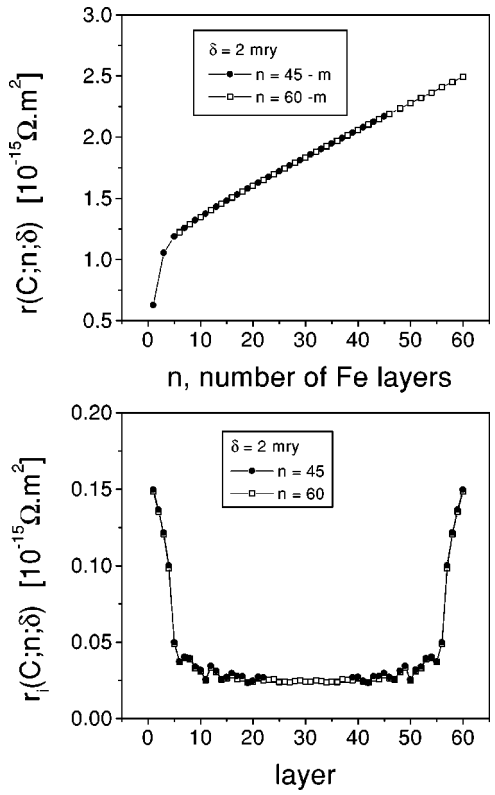

FIG. 3. Top: Variation of the sheet resistance $r(\mathcal{C};n;\delta)$, where $\delta=2$ m Ry, for ferromagnetic bcc Fe(100)/Fe$_n$/Fe with respect to $n=N-m$ for $N=45$ and 60. Bottom: Layer-resolved sheet-resistances $r(\mathcal{C};n;\delta)$ for $n=45$ and 60.

$$k_2(\mathcal{C};n)=\frac{1}{n}\,\frac{r(\mathcal{C};n;\delta_2)-r(\mathcal{C};n;\delta_1)}{\Delta},\quad \Delta=\delta_2-\delta_1, \tag{13}$$

i.e.,

$$r(\mathcal{C};n;\delta)=r_0(\mathcal{C};n)+n\,\delta k_2(\mathcal{C};n), \tag{14}$$

where as will become clear in a moment the constant $k_2(\mathcal{C};n)$ is chosen to be normalized per layer.

Now combining Eqs. (12) and (14), one obtains

$$r_0(\mathcal{C};\delta)=r_0(\mathcal{C};n)+n\Phi(\delta), \tag{15}$$

where

$$\Phi(\delta)=\delta k_2(\mathcal{C};n)-k_1(\mathcal{C};\delta). \tag{16}$$

By taking the limit of $\delta\to 0$ it is easy to see that demanding

$$r_0(\mathcal{C};n)=\lim_{\delta\to 0} r_0(\mathcal{C};\delta) \tag{17}$$

in turn implies that

$$\lim_{\delta\to 0} k_1(\mathcal{C};\delta)=0, \tag{18}$$

since $\delta k_2(\mathcal{C};n)$ trivially vanishes for $\delta\to 0$. In the lower part of Fig. 4, $k_1(\mathcal{C};\delta)$ is linearly extrapolated to $\delta=0$. As can be seen, $k_1(\mathcal{C};\delta)$ indeed tends to zero for $\delta\to 0$. The very small remainder of $0.003.10^{-15}$ Ω m^2 of $k_1(\mathcal{C};\delta)$ at $\delta=0$ has to

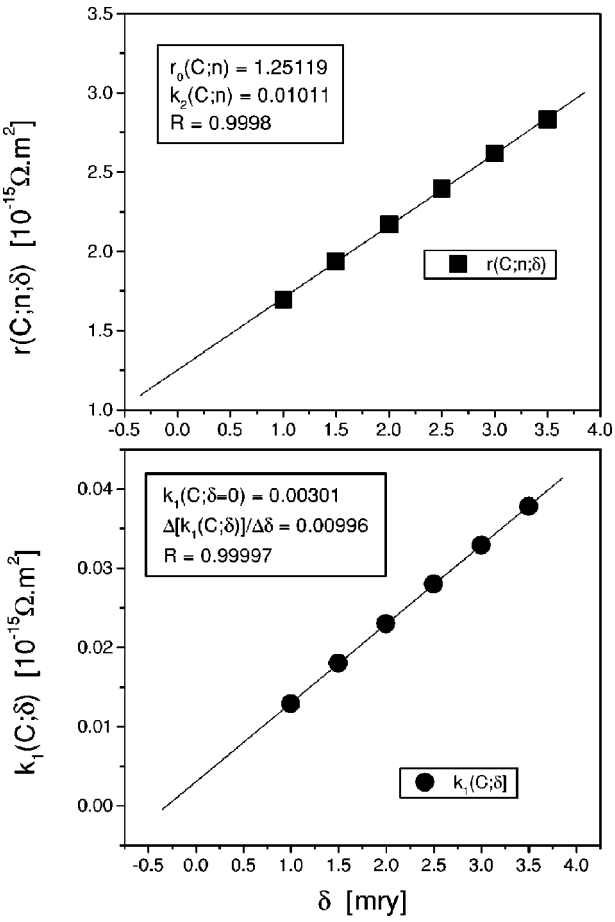

FIG. 4. Top: Variation of $r(\mathcal{C};n;\delta)$ for Fe(100)/Fe$_{45}$/Fe with respect to δ. The linear fit is shown as a full line. Bottom: Variation of $k_1(\mathcal{C};\delta)$ with respect to δ for the same system. R refers to the quality of fitting.

be regarded as the numerical error of the applied procedure. Furthermore, the slope of $k_1(\mathcal{C};\delta)$ with respect to δ is very close to the value of $k_2(\mathcal{C};n)$. Assuming for a moment that $\Phi(\delta)\sim 0$ yields an approximate relation between the two slopes $k_1(\mathcal{C};\delta)$ and $k_2(\mathcal{C};n)$,

$$\delta k_2(\mathcal{C};n)\sim k_1(\mathcal{C};\delta). \tag{19}$$

3. Resistivity and boundary condition at $n\to\infty$

From Eqs. (12) and (17) it follows that for $n\geqslant n_0$

$$\lim_{\delta\to 0} r(\mathcal{C};n+m;\delta)=r_0(\mathcal{C};n)\equiv r_0(\mathcal{C}),\quad m,n\in\mathbb{N}^+, \tag{20}$$

which, however, is nothing but the Cauchy convergence criterion for the sheet resistance demanded in Eq. (7):

$$\lim_{\delta\to 0}[r(\mathcal{C};n+m;\delta)-r(\mathcal{C};n;\delta)]=0,\quad m,n\in\mathbb{N}^+,\quad n\geqslant n_0. \tag{21}$$

Quite clearly, since $r_0(\mathcal{C})$ is a constant, for a pure metal by performing the limit $n\to\infty$ this leads to a correct resistivity $\rho_{CPP}(\mathcal{C})$,

$$\rho_{CPP}(\mathcal{C}) = \lim_{n\to\infty}\left[\frac{r_0(\mathcal{C})}{L}\right] = \frac{r_0(\mathcal{C})}{d}\lim_{n\to\infty}\frac{1}{n} = 0, \tag{22}$$

where d is the interplanar distance. For a substitutionally disordered alloy $r(\mathcal{C};n;\delta)$ has to vary with respect to n in the following manner [also see Eq. (12)]:

$$r(\mathcal{C};n;\delta) = r_0(\mathcal{C};\delta) + n[k_1(\mathcal{C};\delta) + \overline{k}_1(\mathcal{C};\delta)], \quad n \geqslant n_0, \tag{23}$$

where

$$\overline{k}_1(\mathcal{C}) = \lim_{\delta\to 0}\overline{k}_1(\mathcal{C};\delta) \tag{24}$$

is simply the resistivity caused by disorder. In general $\rho_{CPP}(\mathcal{C})$ is therefore given by

$$\rho_{CPP}(\mathcal{C}) = \frac{1}{d}\lim_{\delta\to 0}\left\{\lim_{n\to\infty}\frac{r(\mathcal{C};n;\delta)}{n}\right\}. \tag{25}$$

B. Heterostructures

Since the case of pure leads was discussed in quite some detail, the case of heterostructures, e.g., of the type $\mathrm{Fe}(100)/\mathrm{Fe}_n X_s \mathrm{Fe}_n/\mathrm{Fe}(100)$, where X is the spacer element, is almost trivial, provided the leads and the spacer share the same parent lattice. For $n \geqslant n_0$ and a given value of δ the sheet resistance $r(\mathcal{C};2n+s;\delta)$ varies linearly with respect to n:

$$k_1(\mathcal{C};\delta) = \frac{r(\mathcal{C};2(n+m)+s;\delta) - r(\mathcal{C};2n+s;\delta)}{2m},$$

$$m,n,s \in \mathbb{N}^+, \quad n \geqslant n_0, \tag{26}$$

i.e.,

$$r(\mathcal{C};2(n+m)+s;\delta) = r(\mathcal{C};2n+s;\delta) + 2mk_1(\mathcal{C};\delta). \tag{27}$$

The relevant part of the heterostructure is therefore simply defined by the condition that by using a finite δ for $n \geqslant n_0$ the sheet resistance starts to grow linearly in n, i.e.,

$$r(\mathcal{C};2n_0+m+s) = \lim_{\delta\to 0} r(\mathcal{C};2n_0+s;\delta), \quad m,n,s \in \mathbb{N}^+ \tag{28}$$

remains constant with respect to m. It should be noted that the necessity to use a finite imaginary part of the Fermi energy, which at the beginning seemed to be like an unwanted complication, turns out to be of practical importance in the case of heterostructures since the number of lead layers has to be increased only until the described linear behavior is reached.

The magnetoresistance ratio of the relevant part of the heterostructure is then defined by

$$R = \frac{r(\mathcal{AP};2n_0+s) - r(\mathcal{P};2n_0+s)}{r(\mathcal{AP};2n_0+s)}, \tag{29}$$

and can be approximated by

TABLE I. Investigated systems.

System A	System B	System C
Homogeneous alloying	Interdiffusion and ordering	Alloying and ordering
bcc bulk Fe	bcc bulk Fe	bcc bulk Fe
Fe_{12}	Fe_{12}	Fe_{12}
Ge_cVac_{1-c}	$Ge_{1-c}Vac_c$	Vac
Ge_cVac_{1-c}	Ge_cVac_{1-c}	Ge_cVac_{1-c}
Ge_cVac_{1-c}	$Ge_{1-c}Vac_c$	Vac
Ge_cVac_{1-c}	Ge_cVac_{1-c}	Ge_cVac_{1-c}
⋮	⋮	⋮
⋮	⋮	⋮
Ge_cVac_{1-c}	Ge_cVac_{1-c}	Ge_cVac_{1-c}
Ge_cVac_{1-c}	$Ge_{1-c}Vac_c$	Vac
Ge_cVac_{1-c}	Ge_cVac_{1-c}	Ge_cVac_{1-c}
Ge_cVac_{1-c}	$Ge_{1-c}Vac_c$	Vac
Fe_{12}	Fe_{12}	Fe_{12}
bcc bulk Fe	bcc bulk Fe	bcc bulk Fe

$$R(\delta) = \frac{r(\mathcal{AP};2n_0+s;\delta) - r(\mathcal{P};2n_0+s;\delta)}{r(\mathcal{AP};2n_0+s;\delta)}, \tag{30}$$

where $\mathcal{P}$ and $\mathcal{AP}$ refer to the parallel and antiparallel magnetic configurations, respectively. Assuming for a moment that $k_2(\mathcal{AP};2n_0+s) \sim k_2(\mathcal{P};2n_0+s)$ [see Eq. (14)], implies that

$$R > R(\delta). \tag{31}$$

III. APPLICATIONS TO Fe/Ge HETEROSTRUCTURES

All calculations reported here refer to a bcc parent lattice[15] with a lattice spacing corresponding to that of bcc Fe ($a_0 = 7.27$ a.u.). In Table I we show the composition of three kinds of Fe/Ge heterostructures we have studied by using the CPA.[12]

System A: 12 layers of a homogeneous alloy of Ge and vacancies (Vac), (Ge_cVac_{1-c}), sandwiched between 12 layers of Fe matched to bcc Fe leads. For the case of a pure Ge spacer we also vary the number of Ge layers.

System B: In this type of system the spacer is 15 layers thick and consists of alternating (Ge_cVac_{1-c}) and ($Ge_{1-c}Vac_c$) layers, such that for $c=1$ pure vacuum layers are at the interfaces with the Fe electrodes, i.e., only every second plane is a plane of Ge atoms, while every other plane is empty (Vac). By varying the Ge concentration in the interval $0.5 \leqslant c \leqslant 1$ one can follow physical properties from a statistically disordered spacer at $c=0.5$ to the completely ordered case at $c=1$.

System C: Again 15 spacer layers are considered, but now only every other layer is an alloyed plane of Ge and vacancies, while the remaining spacer layers are empty (pure vacancy planes). By varying the Ge concentration one can trace the change in physical properties when the planes containing Ge are separated by twice the interlayer distance of bcc Fe.

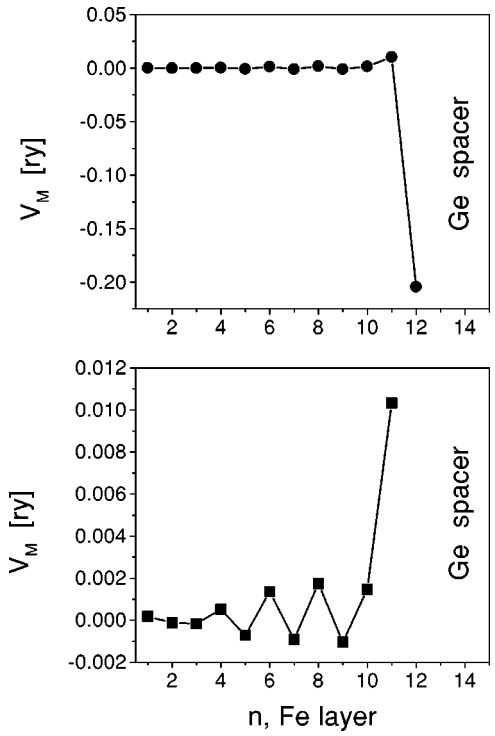

FIG. 5. Layer-resolved Madelung potentials for the Fe layers next to the Fe/Ge interface in bcc $Fe(100)/Fe_{12}Ge_9Fe_{12}/Fe$. The bottom figure shows the oscillations of the Madelung potentials into the interior of the Fe leads on an enlarged scale.

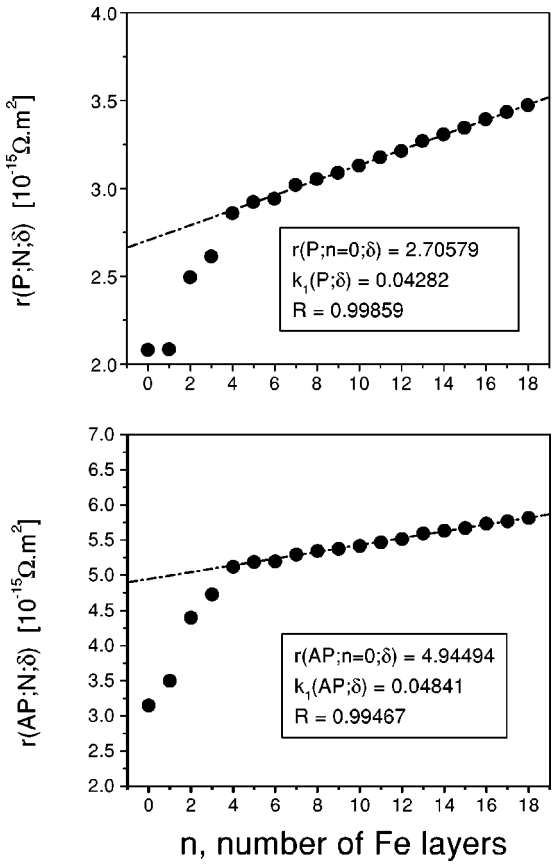

FIG. 6. Variation of the sheet resistance $r(\mathcal{C};n;\delta)$, $\delta=2$ m Ry, for bcc $Fe(100)/Fe_nGe_sFe_n/Fe$, $\delta=2$ m Ry, $s=9$, with respect to n. The upper panel refers to the parallel configuration, and the lower to the antiferromagnetic configuration. Dashed lines indicate the extrapolation of the linear regime to $n=0$.

At $c=0.5$ on the average only every second atomic position is occupied by Ge. Clearly enough for $c=1$ one recovers the ordered structure of system B.

A. Layer dependence of the Madelung potentials

In Fig. 5 we show the layer-dependent Madelung potentials of the first 12 Fe layers neighboring the Ge spacer in the heterostructure: $Fe(100)/Fe_{12}Ge_9Fe_{12}/Fe$. From the enlarged scale at the bottom of this figure we see that the ''Friedel'' oscillations into the interior of the electrodes extend over more than nine Fe layers. It is these Madelung potentials which tell us about the redistribution of charge in our heterostructure. Therefore in order to include these small variations in the charge density the number of layers N_0 to be determined self-consistently should be at least nine whenever possible. Figure 5 thus answers the first question posed in Sec. I, namely, the question of how many lead layers (N_0) have to be considered in terms of the underlying electronic structure.

B. Layer dependence of the sheet resistance

Figure 6 shows the sheet resistance $r(\mathcal{C};2n+s;\delta)$ for the heterostructure $Fe(100)/Fe_nGe_sFe_n/Fe$, $\delta=2$ m Ry, $s=9$, with respect to the number of Fe layers n for the parallel (top) and the antiparallel magnetic configuration (bottom). As can be seen from this figure for both configurations linear behavior in n sets in for $n\geqslant 9$. In terms of electric transport the minimum number of lead layers that has to be included is therefore at least $n_0=9$ (the second question raised in the introduction). It should be noted that the slopes in Fig. 6 normalized per Fe layer are very close to the value for $\delta=2$ m Ry in Fig. 2. This again demonstrates the validity of our approach.

For the heterostructure corresponding to $s=9$ and $n=18$, in Fig. 7 the layer-resolved sheet resistances corresponding to the parallel magnetic configuration are displayed together with the corresponding quantities for the pure Fe system, $Fe(100)/Fe_{45}/Fe$. Here one can see that in the first and last nine layers of the heterostructure the layer-resolved sheet resistances are very close to those in pure Fe. Comparing this figure with the bottom part of Fig. 3 reveals that the origin of the linear behavior of $r(\mathcal{C};2n+s;\delta)$ with respect to $n\geqslant n_0$ is the same as for the lead part only. However, since in the Fe-only system the Madelung potentials are exactly zero in each layer, n_0 and N_0 (see Sec. III) are in general different and have to be determined independently.

The layer-resolved sheet resistance $r_i(\mathcal{C};n;\delta)$ in Fig. 7 is about five times larger in the Ge spacer than in the bulk of the Fe layers. We can conclude that while bcc Ge with a lattice constant of Fe is more resistive than a good metal, there is no indication that the conduction is not metallic. The other notable feature in Fig. 7 is the oscillations of the $r_i(\mathcal{C};n;\delta)$ about the Fe/Ge interface. While the total resistance must be positive, the negative r_i indicate regions where

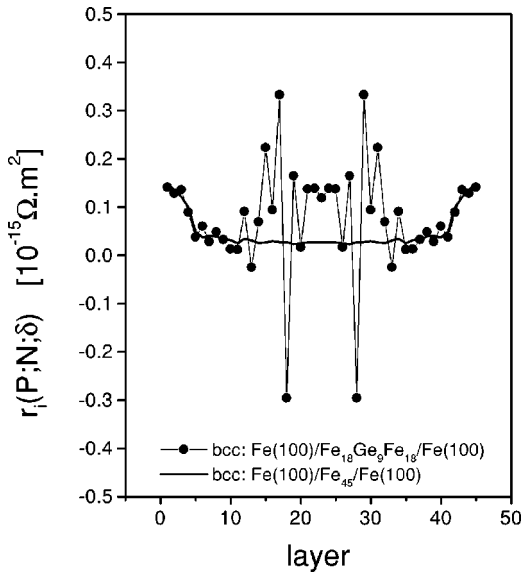

FIG. 7. Layer-resolved sheet resistance $r_i(\mathcal{C};n;\delta)$, $\delta=2$ m Ry, for bcc Fe(100)/$Fe_{18}Ge_9Fe_{18}$/Fe, $\delta=2$ m Ry. As a comparison, the case for Fe(100)/Fe_{45}/Fe (full line) is shown.

the electric field opposes (slows down) CPP transport so as to maintain steady-state current across the entire heterostructure. In all the cases reported in the following, the number of Fe lead layers is fixed to $n_0=N_0=12$, which definitely meets both requirements, and an imaginary part of the Fermi energy of $\delta=2$ m Ry is used.

C. Magnetoresistance in Fe/Ge heterostructures

For all three types of systems (see Fig. 8), one and the same conclusion can be drawn: a sizable $R(\delta)$ can be expected only very close to the ordered structures, namely, for $c\geqslant 0.9$. The reason for this strong dependence of the $R(\delta)$ ratio on the vacancy concentration becomes evident by inspecting Fig. 9: the sheet resistance for the antiparallel configuration, which is quite a bit larger than that for the parallel configuration for $c=1$, immediately drops as soon as vacancies are present. Below 90% Ge both sheet resistances, parallel and antiparallel, have the same values. This particular feature applies to all three types of systems we have studied.

In the upper panel of Fig. 10 we show the variation of $R(\delta)$ for Fe/$Fe_{12}Ge_sFe_{12}$/Fe with respect to the number s of

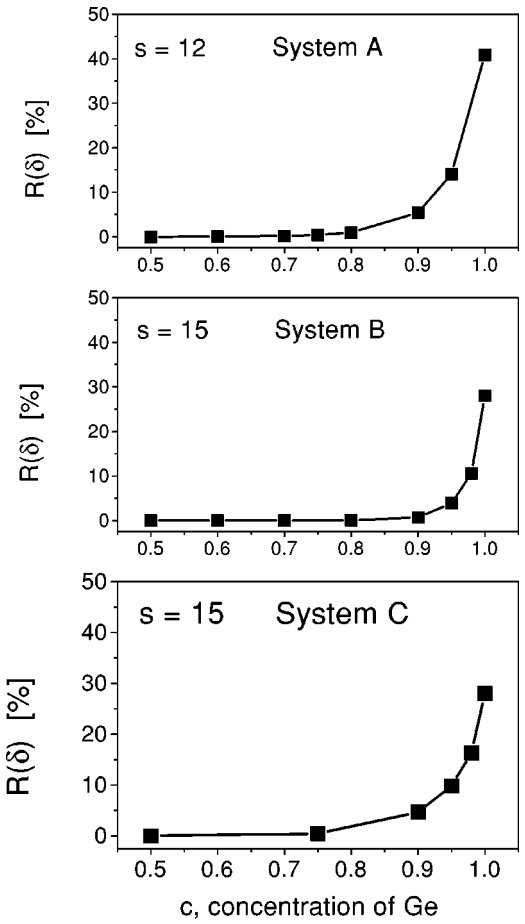

FIG. 8. Calculated magnetoresistance for the three types of spacer considered, see Table I. The number of spacer layers is indicated, $\delta=2$ m Ry.

Ge layers. As can be seen by going from 6 to 21 spacer layers $R(\delta)$ varies between about 45% and 35%; in the lower part of Fig. 10 the variation of the $R(\delta)$ of Fe/$Fe_nGe_9Fe_n$/Fe with respect to the number of n Fe layers considered to be part of the electrodes is displayed. *Grosso modo*, it can be stated that for a given ordered structure, the magnetoresistance is rather insensitive to n as long as there are at least 2–3 such layers considered to be part of the heterostructure.

In addition to the cases listed in Table I, we also studied the effect of interdiffusion at the Fe/Ge interface in terms of the system:

$$\mathrm{Fe}(100)/\mathrm{Fe}_{11}/(\mathrm{Fe}_c\mathrm{Ge}_{1-c})/(\mathrm{Fe}_{1-c}\mathrm{Ge}_c)/\mathrm{Ge}_{10}/(\mathrm{Fe}_{1-c}\mathrm{Ge}_c)/(\mathrm{Fe}_c\mathrm{Ge}_{1-c})/\mathrm{Fe}_{11}/\mathrm{Fe}$$

i.e., by interdiffusing those two layers in the Fe(100)/$Fe_{12}Ge_{12}Fe_{12}$/Fe system that form the interfaces. The top part of Fig. 11 shows the sheet resistances $r(\mathcal{C};2n+s;\delta)$ for these kinds of systems with respect to the interdiffusion concentration c; in the lower part the corresponding magnetoresistance (MR) is displayed. As can be seen, the effect of interdiffusion is almost dramatic: only 5% interdiffusion halves the magnetoresistance characteristic for the ordered system. As in all other cases shown (see Figs. 8 and 9), the immediate drop of $r(\mathcal{AP};2n+s;\delta)$ in the presence of interdiffusion causes this effect.

Finally we want to address the question of where the mag-

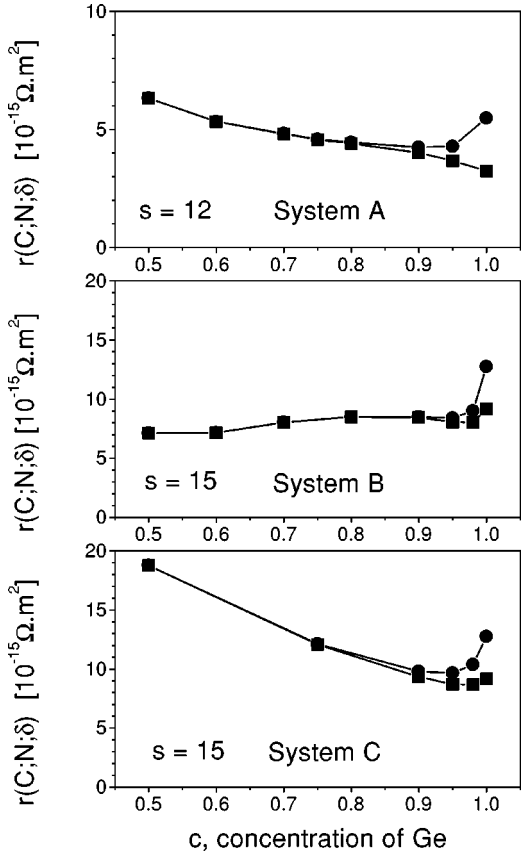

FIG. 9. Calculated sheet resistances for the three types of spacer considered, see Table I. Squares and circles refer to the parallel and antiparallel configuration, respectively. The number of spacer layers is indicated, $\delta = 2$ m Ry.

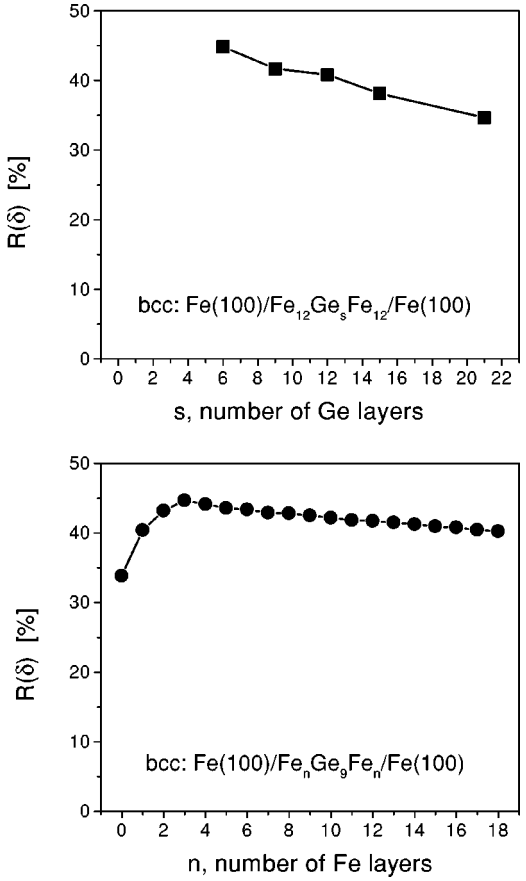

FIG. 10. Top: Variation of the magnetoresistance in bcc $Fe(100)/Fe_{12}Ge_sFe_{12}/Fe$ with respect to the number of Ge layers s. Bottom: Variation of the magnetoresistance in bcc $Fe(100)/Fe_nGe_9Fe_n$ /Fe, $N = 18$, with respect to n. In both entries, $\delta = 2$ m Ry.

netoresistance comes from. For this purpose one can define the following layer-resolved magnetoresistances $R_i(\delta)$ ratio,

$$R_i(\delta) = \frac{1}{r(\mathcal{AP};2n+s;\delta)} \times [r_i(\mathcal{AP};2n+s;\delta) - r_i(\mathcal{P};2n+s;\delta)], \quad (32)$$

which, of course, summed over the layer index i yields $R(\delta)$. In Fig. 12 these layer-resolved magnetoresistances are shown for the system $Fe(100)/Fe_{12}Ge_sFe_{12}/Fe$, $s = 12$ and 21. As can be seen from this figure the magnetoresistance essentially arises from the first 3–4 Fe layers next to the spacer, the contributions from the spacer part of the system are rather small. This confinement of the CPP MR to a few Fe layers next to the interface is similar to that found for CIP MR; among other things it explains very nicely both parts of Fig. 10; i.e., the decrease of the MR as we increase either the number of spacer or electrode layers.

IV. CONCLUSION

In this paper we studied perpendicular, or CPP, transport in metallic heterostructures in terms of the Kubo-Greenwood approach for layered systems in a fully relativistic spin-polarized mode. We first dealt with a description of how to subtract the resistance of the leads from the structure itself. There are two different issues one needs to delineate: (1) How many layers of lead material have to be considered in the self-consistent solution of the electronic structure to accurately determine the charge and spin redistribution (the Madelung potentials) arising from the varying electronic properties of the layers. As seen from the oscillations of the layer-resolved Madelung potentials into the interior of the leads (see Fig. 4), we showed the necessity to include about $N_0 = 9$ layers of the electrode material next to the metal-nonmetal interface. (2) How many layers n_0 of lead material have to be considered in the calculation of transport properties (the size of the conductivity matrix to be inverted) so as to properly account for the charge and spin accumulation when the current is driven across the region with the charge and spin redistribution so as to obtain a resistance that is independent of the number of lead layers chosen.

For a proper splicing of the region of interest from the leads one has to do it in a region where the electric field due to the redistribution effects vanishes. This problem is common to the Kubo and Landauer approaches when they are used to describe metallic conduction across interfaces with the attendant charge and spin accumulation; therefore, we

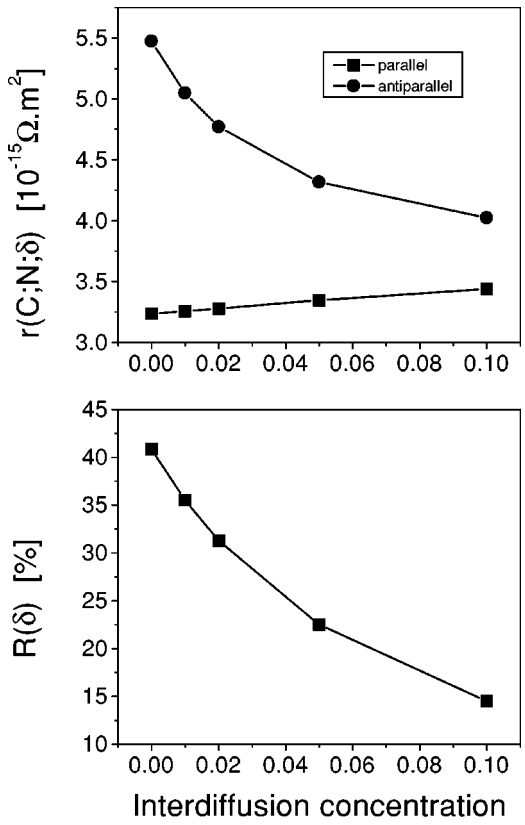

FIG. 11. Parallel and antiparallel sheet resistance $r(\mathcal{C};n;\delta)$ (top) and $R(\delta)$ for interdiffused bcc $Fe(100)/Fe_{12}Ge_{12}Fe_{12}/Fe$, $\delta = 2$ m Ry.

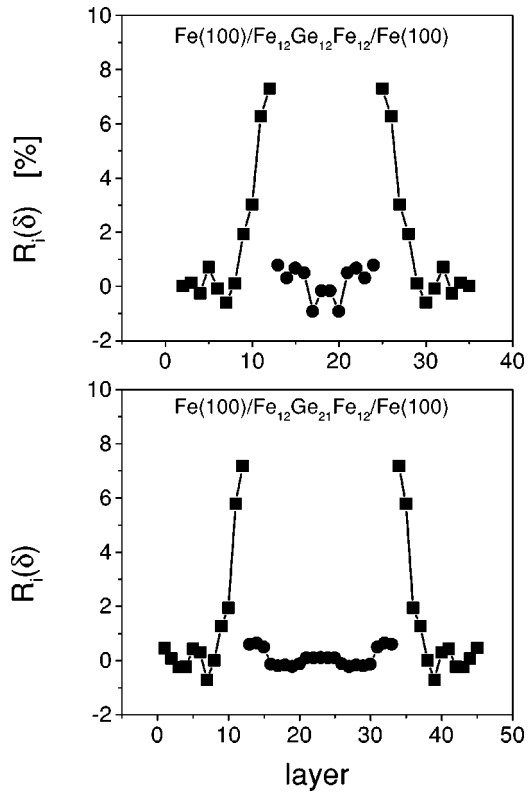

FIG. 12. Layer-resolved magnetoresistance $R_i(\mathcal{C};n;\delta)$, $\delta = 2$ m Ry, for the parallel configuration of bcc $Fe(100)/Fe_sGe_{12}Fe_{12}/Fe$ (top) and bcc $Fe(100)/Fe_sGe_{21}Fe_{12}/Fe$ (top). Squares refer to Fe layers, and circles to Ge layers.

now have a prescription for calculating CPP magnetotransport in magnetically layered structures. Our approach of using the Kubo formalism for CPP has the advantage over the Landauer-Büttiker formalism, as we can use CPA to deal with defect scattering, in particular interdiffusion at the interfaces. While the Kubo formalism entails vertex corrections they are no more important (worrisome) than those entering CIP. The problem of current driven accumulation does not present itself in magnetic tunnel junctions as the current density is extremely small compared to that in metallic structures; for this reason the Caroli formalism, which is able to calculate the resistance for any part of a structure, was used in our recent paper on tunneling conductance.[3]

The sheet resistances we calculated for the Fe/Ge heterostructures are in part due to our using a finite imaginary part (δ) of the Fermi energy. Clearly enough, for a restricted number of well-defined systems one can numerically perform the $\delta \rightarrow 0$ limit; see, e.g., Fig. 3. For the large number of different systems shown in Figs. 7–10 this is not possible at the present time, and is perhaps also of less interest since in the first place only characteristic (qualitative) features with respect to system parameters such as thickness dependences, interdiffusion, interlayer distances, etc., matter.

For the three types of Fe/Ge heterostructures we studied, existence of a sizable MR; as few as 5% vacancies causes the MR ratio to plummet. This corresponds also to the interdiffusion study shown in Fig. 10. With different structures in the bcc (100) Ge spacer, we find that the concentration of vacancies plays a crucial role for the existence of a sizable magnetoresistance, while the actual structure in the spacer seems to be of less importance. This was demonstrated in particular in terms of layer-resolved magnetoresistances, which proved that the magnetoresistance effect is essentially confined to 3–4 Fe layers next to the spacer.

This paper provides a method for calculating the CPP resistances and MR in metallic multilayered structures; it uses the results obtained for the conductivity in the direction of layer growth, and shows how to properly invert them to obtain resistances. For the spacer used and the thicknesses considered our results are not very relevant to any experiments on ''real'' tunnel junctions as the conductions seems to remain metallic across the spacer layer, at least for spacer thicknesses up to 21 ML. Furthermore, since Fig. 12 suggests that the magnetoresistance is mainly caused by the interfaces, the actual structure in the interior of the spacer part seems to be perhaps less important than generally believed.

ACKNOWLEDGMENTS

We thank Professor P. M. Levy and Professor I. Mertig for many extremely useful discussions. This paper resulted from a collaboration partially funded by the TMR network ''Interface Magnetism'' (Contract No. EMRX-CT96-0089) and the RTN network ''Magnetoelectronics'' (Contract No. RTN1-

1999-00145). Financial support was also provided by the Center for Computational Materials Science (Contract No. GZ 45.442), the Austrian Science Foundation (Contract Nos. P12146, P12352, and T27-TPH), the Hungarian National Science Foundation (Contract No. OTKA T030240 and T029813). We also wish to thank the computing center IDRIS at Orsay as part of the calculations was performed on their Cray T3E machine.

[1] P. M. Levy, in *Solid State Physics*, edited by H. Ehrenreich and D. Turnbull (Academic, Cambridge, MA, 1994), Vol. 47, pp. 367–462.

[2] P. M. Levy and I. Mertig, in *Spin-Dependent Transport in Magnetic Nanostructures*, edited by T. Shinjo and S. Maekawa (Gordon and Breach, New York, 2000).

[3] P. M. Levy, K. Wang, P. H. Dederichs, C. Heide, and L. Szunyogh, Philos. Mag. B (to be published).

[4] H. E. Camblong, P. M. Levy, and S. Zhang, Phys. Rev. B **51**, 16 052 (1995).

[5] D. S. Fisher and P. A. Lee, Phys. Rev. B **23**, 6851 (1981).

[6] J. Banhart, H. Ebert, P. Weinberger, and J. Voitländer, Phys. Rev. B **50**, 2104 (1994).

[7] A. Vernes (private communication).

[8] P. Walser, M. Schleberger, P. Fuchs, and M. Landolt, Phys. Rev. Lett. **80**, 2217 (1998).

[9] L. Szunyogh, B. Újfalussy, and P. Weinberger, Phys. Rev. B **51**, 9552 (1995).

[10] B. Újfalussy, L. Szunyogh, and P. Weinberger, Phys. Rev. B **54**, 9883 (1996); **55**, 14 392 (1997); L. Szunyogh, B. Újfalussy, C. Blaas, U. Pustogowa, C. Sommers, and P. Weinberger, *ibid.* **56**, 14 036 (1997); J. Zabloudil, C. Uiberacker, U. Pustogowa, C. Blaas, L. Szunyogh, C. Sommers, and P. Weinberger, *ibid.* **57**, 7804 (1998); C. Uiberacker, J. Zabloudil, P. Weinberger, L. Szunyogh, and C. Sommers, Phys. Rev. Lett. **2**, 1289 (1999); for a review, see P. Weinberger, and L. Szunyogh, Comput. Mater. Sci. **17**, 414 (2000).

[11] J. Zabloudil, L. Szunyogh, U. Pustogowa, C. Uiberacker, and P. Weinberger, Phys. Rev. B **58**, 6316 (1998).

[12] P. Weinberger, P. M. Levy, J. Banhart, L. Szunyogh, and B. Újfalussy, J. Phys.: Condens. Matter **8**, 7677 (1996).

[13] C. Blaas, P. Weinberger, L. Szunyogh, P. M. Levy, and C. Sommers, Phys. Rev. B **60**, 492 (1999).

[14] C. Blaas, L. Szunyogh, P. Weinberger, C. Sommers, and P. M. Levy, Phys. Rev. B **63**, 224408 (2001).

[15] P. Weinberger, Philos. Mag. B **75**, 509 (1997).